Sequence-Specific Assignments of the ^1H Nuclear Magnetic Resonance Spectra of Reduced High-Potential Ferredoxin (HiPIP) from *Chromatium vinosum*

Jacques Gaillard,*,‡ Jean-Pierre Albrand,§,∥ Jean-Marc Moulis,⊥ and David E. Wemmer#

DRFMC-SESAM-SCPM, DBMS-RMBM, and DBMS-MEP, 85X CENG, 38041 Grenoble Cedex, France, and Department of Chemistry, University of California, Berkeley, California 94720

Received February 18, 1992; Revised Manuscript Received March 23, 1992

ABSTRACT: The ^1H resonances of the high-potential $[4Fe-4S]^{2+}$ ferredoxin from *Chromatium vinosum* have been assigned through conventional sequential methodology applied to 2D NMR spectra. Almost 80% of the residues were identified using standard 2D COSY, HOHAHA, and NOESY pulse sequences. These residues correspond to four segments of the primary structure that do not interact strongly with the iron–sulfur cluster. A minor correction to the amino acid sequence is strongly suggested by these NMR data. Additional protons more sensitive to the proximity of the cluster were assigned by a combination of NOESY experiments with fast repetition rates and short mixing times and of HOHAHA spectra recorded with reduced spin-lock duration aimed at compensating for the short relaxation rates. Hence, the contributions of 79 residues out of 85 were identified in NMR spectra, among which the assignments of 64 residues were completed. Even the fastest relaxing protons, like those of the cysteine ligands, could be correlated, partly because the strong hyperfine shifts isolate them from the crowded diamagnetic region. However, other protons, in particular those involved in NH–S hydrogen bonds with the iron–sulfur cluster, were more difficult to identify, most probably because their relatively broad signals overlapped with those of protons not or less perturbed by the active site. The availability of the major part of the ^1H NMR assignments has enabled the detection and identification of many interresidue NOESY cross peaks. These data are in full agreement with the elements of secondary structure previously revealed by X-ray crystallographic analysis of the protein. Moreover, the general folding of *C. vinosum* high-potential ferredoxin studied here in solution differs only slightly from that provided by the X-ray crystallographic structure.

A large number of enzymes and electron-transfer proteins contain [4Fe–4S] clusters at their active site. In ferredoxins, the inorganic core usually cycles between the 1+ and 2+ formal charges, hence allowing the protein to exchange electrons at low potential, in the −250 to −650 mV range versus NHE.[1] A distinct class of small (ca. 60–85 amino acids) proteins is set apart as its active center is organized around a [4Fe–4S] cluster of similar structure which switches between the 2+ and 3+ redox levels at potentials measured in the +50 to 400 mV range vs NHE. These proteins are most probably implicated as electron transfer-only agents and are generally isolated from phototrophic bacteria (Tedro et al., 1985). They have received the trivial name of HiPIP for high-potential iron–sulfur proteins. The structure of the [4Fe–4S] cluster determined by X-ray crystallography is identical in the low-potential and high-potential ferredoxins (Carter, 1977). The reasons for the different redox transitions in the two types of ferredoxins have been extensively discussed (Carter, 1977; Backes et al., 1991) and have converged on the higher hydrophobic environment, the lower number of hydrogen bonds to sulfur ligands, and the limited solvent accessibility of the cluster in the case of HiPIPs.

Most of our knowledge on the structure of HiPIPs comes from two X-ray crystallographic studies on the proteins from *Chromatium vinosum* (Carter et al., 1974) and *Ectothiorhodospira halophila* (Breiter et al., 1991). These results provided a detailed picture of the molecular organization around the [4Fe–4S] cluster and have stimulated intense research to unravel the electron-transfer mechanism obeyed by these proteins. However, mainly because X-ray crystallography is applied on crystals and retains relatively little information on the dynamics of the system, the principal determinants in the redox properties of HiPIPs remain unidentified. Some hints about the changes affecting the active site upon electron exchange have been obtained through the use of various techniques such as Mössbauer spectroscopy (Middleton et al., 1980), NMR of the paramagnetically shifted protons (Nettesheim et al., 1983; Krishnamoorthi et al., 1986, 1989; Cowan & Sola, 1990; Bertini et al., 1991, 1992), circular dichroism (Przysiecki et al., 1985), and resonance Raman spectroscopy (Moulis et al., 1988; Backes et al., 1991). However, much remains to be learned about the contribution of the polypeptide chain to the process.

When applied to proteins, 2D NMR techniques can provide a wealth of structural information on the molecule in solution (Wüthrich, 1986); in addition, the dynamic and electronic properties can be probed, a particularly useful feature in the case of paramagnetic proteins (Dugad et al., 1990). As a first step toward such a study with reduced *C. vinosum* HiPIP, the ^1H NMR assignments for 79 residues out of 85 are presented here. They complement the on-going studies on the assign-

* Author to whom correspondence should be addressed.
‡ DRFMC-SESAM-SCPM.
§ DBMS-RMBM.
∥ Member of the Centre Nationale de la Recherche Scientifique.
⊥ DBMS-MEP.
University of California, Berkeley.

[1] Abbreviations: COSY, correlated spectroscopy; DQF-COSY, double-quantum filtered correlated spectroscopy; FID, free induction decay; HOHAHA, homonuclear Hartmann–Hahn spectroscopy; HiPIP, high-potential iron–sulfur protein; NHE, normal hydrogen electrode; NOE, nuclear Overhauser effect; NOESY, nuclear Overhauser enhancement spectroscopy.

0006-2960/92/0431-5632$03.00/0

ments of the hyperfine-shifted protons in the same protein (Bertini et al., 1992).

Materials and Methods

Protein Purification. Large-scale (20-L) cultures of *C. vinosum* DSM 180 (type strain) were inoculated from photoautotrophic precultures and grown photoheterotrophically with malate as carbon source (Malik, 1983). [4Fe–4S] high-potential ferredoxin was purified from batches of ca. 150 g of cells as follows. The cell pellet was suspended in 750 mL of 0.2 M Tris-HCl, pH 7.4 (buffer A) and sonicated for 7 min at high power while keeping the solution temperature below 30 °C. Cell debris were removed by centrifugation at 4 °C (75 min, 12000*g*), and the resulting supernatant was further centrifuged at 4 °C (3 h, 300000*g*). The brown-orange supernatant was loaded on a 50-mL DEAE-cellulose column (DE-52, Whatman, U.K.) equilibrated with buffer A and extensively washed with the same buffer until no protein material was eluted. The fraction which did not bind to the anion exchange column was fractionated by ammonium sulfate precipitation between 50% and 90% saturation at 4 °C. The 90% pellet was suspended in 100 mL of buffer A and dialyzed in Spectra-Por 3 (Spectrum Medical Industries Inc., Los Angeles, CA) against 40 volumes of 1 mM Tris-HCl, pH 8.0 (buffer B). After three buffer changes, the solution not crossing the dialysis tube was loaded on a 20-mL DE-52 column equilibrated in buffer B. The HiPIP fraction was eluted with buffer B containing 0.1 M NaCl and concentrated on an Amicon YM5 membrane. It was further purified by gel filtration through a 500-mL Sephadex G-50 column equilibrated with 10 mM potassium phosphate buffer, pH 7.5. The most retarded, brown band was then loaded on a small DE-52 column equilibrated with the same phosphate buffer and developed with a 0–0.1 M NaCl linear gradient. The HiPIP solution was concentrated on an Amicon YM5 membrane and filtrated through a 500-mL AcA 202 (IBF Biotechnics, Villeneuve-la-Garenne, France) column equilibrated with 10 mM potassium phosphate buffer, pH 7.5. The brown fraction containing HiPIP displayed an electronic absorption spectrum with a well-defined relative maximum at 388 nm and an A_{284}/A_{388} ratio of 2.48, indicative of pure holoprotein (Bartsch, 1978).

For NMR measurements, HiPIP solutions were brought to the desired pH (pH 6) with concentrated potassium phosphate buffer and concentrated to 0.4 mL on an Amicon YM5 membrane. For samples in D_2O, this solution was freeze-dried, the protein was solubilized in 100 μL of D_2O (99.8%, CEA-Oris, Gif-Sur-Yvette, France), freeze-dried again, and eventually solubilized in 0.4 mL of D_2O (99.95%, CEA-Oris, Gif-Sur-Yvette, France). The final HiPIP solution in the NMR tubes was about 3 mM with potassium phosphate buffer 0.1 M. Samples dissolved in H_2O contained 15% (v/v) D_2O for the lock.

NMR Spectroscopy. NMR spectra were acquired on a AMX 600 BRUKER spectrometer using a reverse observation probe. Spectra were recorded at five different temperatures (291, 296, 300, 304, and 308 K) to resolve accidental overlaps but only the data obtained at 304 and 308 K have been used in this report, unless otherwise stated. A spectral width of 15625 Hz was used when the paramagnetically shifted protons had to be observed or 9259 Hz in other cases. Chemical shifts were referenced relative to the water resonance set at 4.7 ppm at 308 K.

COSY spectra were recorded in the module mode; DQF-COSY (Rance et al., 1983), HOHAHA (Bax & Davis, 1985), and NOESY (Macura et al., 1981) spectra were recorded in the pure absorption mode using the method of States et al. (1982) to achieve phase-sensitive detection in the t_1 dimension. The water signal was suppressed by low-power selective irradiation during the relaxation period and, in the case of the NOESY and HOHAHA experiments, by a jump–return (Plateau & Guéron, 1982) "reading" pulse replacing the last pulse of the NOESY sequence or following a "flip-back" pulse in the HOHAHA sequence (Bax, 1989). A WALTZ-17 sequence flanked by 2-ms purging pulses (Bax, 1989) was used for HOHAHA mixing times of 30, 50, and 70 ms. Some NOESY experiments designed to emphasize the correlations of the fast-relaxing protons were run with a fast repetition rate (80-ms relaxation recovery following complete saturation by 4 × 2-ms nonselective pulses) and with a short 15-ms mixing time. Two-dimensional arrays of 700–1024 (t_1) × 2048 (t_2) data points were acquired to yield 1024 × 1024 real points matrices after zero-filling and Fourier transformation. Lorentz to Gauss transformation with broadening factors of −15 to −80 Hz were applied to the FID prior to Fourier transformation, and a polynomial baseline correction of second order was systematically applied to the rows of the transformed matrices. The BRUKER software package as well as FELIX (Hare Research Inc.) were used for processing the data.

Results

Sequence-specific resonance assignments were achieved following the conventional method devised by Wüthrich (1986). In a first step, NMR resonances on COSY and HOHAHA spectra were associated with spin systems arising from the different types of amino acids; the number and type of recognized spin systems were in general agreement with the composition of the protein. However, all spin systems expected from *C. vinosum* HiPIP could not be observed, partly because some of them experience broadening through the influence of the paramagnetic iron–sulfur center. Indeed, although this cluster displays a diamagnetic ground spin state in the case of reduced HiPIP, the excited levels are sufficiently populated under the conditions of the NMR experiments as to produce a net electronic spin. This prevents the correlations of the protons in close interaction with the electronic spin to be observed as the magnetization decay through paramagnetic relaxation becomes much faster than the transfer rate through dipolar cross-relaxation or *J*-coupling.

To proceed with resonances assignments, distance connectivities indicated by NOESY experiments served as a guide to align the identified spin systems with the known sequence of the protein (Tedro et al., 1981). All $C^{\alpha}H(i)$–$NH(i+1)$ ($d_{\alpha N}$), $C^{\beta}H(i)$–$NH(i+1)$($d_{\beta N}$), and $NH(i)$–$NH(i+1)$(d_{NN}) cross peaks enabled us to connect the major parts of the protein. As expected, these stretches of sequence were interrupted by prolines and in the regions surrounding the cysteine ligands of the iron–sulfur center (Figure 1).

$C^{\alpha}H(i)$–$NH(i+1)$ correlations were sufficient to identify the main-chain protons of the Ala-4–Arg-33 peptide (Figure 2), except for Arg-28. The NOESY peak between the NH of Val-29 and $C^{\gamma}H$ of Arg-28 at 0.5 ppm was used to locate the latter residue, the protons of which are characterized by unusual chemical shifts (Table I). The signals of the Tyr-19 side chain are broad, most probably because of the proximity to the iron–sulfur cluster. An accidental overlap between the $C^{\alpha}H$ of Gln-21 and the $C^{\alpha}H$ of Lys-83 was noticed, but the connection between residues 21 and 22 was firmly established through the NH(21)–NH(22) and $C^{\beta}H(21)$–NH(22) NOESY cross peaks.

Sequential connectivities have also allowed the assignments of the Gly-35–Leu-36 pair. The Leu-36–Pro-37 connectivity

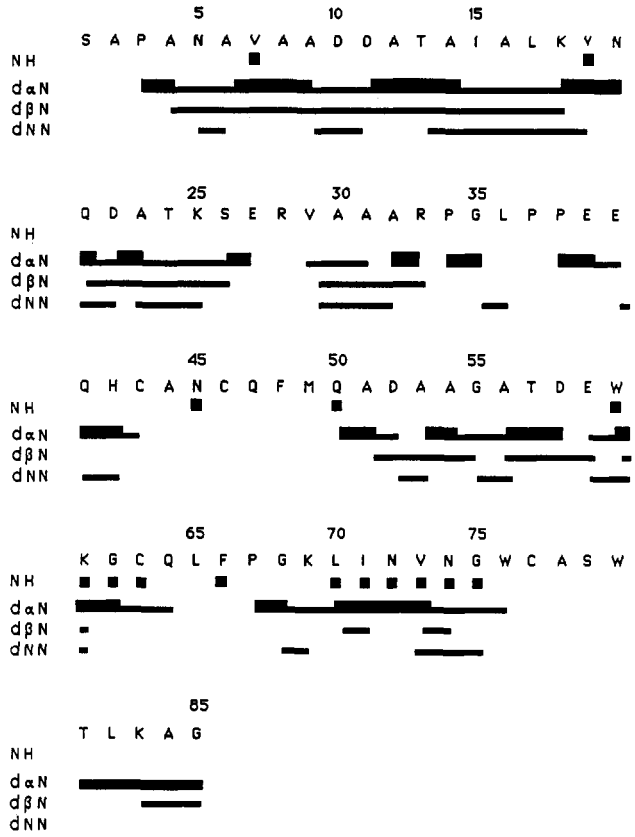

FIGURE 1: Summary of the sequential assignments involving the NH, $C^{\alpha}H$, and $C^{\beta}H$. The NH–$C^{\alpha}H$ NOESY cross peaks recorded with a mixing time of 60 ms have been divided into strong and weak signals according to the height of the bar underneath the sequence. Filled squares indicate slowly exchanging NH protons.

was established through two NOESY cross peaks correlating the $C^{\alpha}H$ of Leu-36 with $C^{\delta}H$ of Pro-37. The Gln-39–His-42 portion and the last two internal segments Gln-50–Gly-62 (Figure 3) and Gly-68–Gly-75 were also identified through sequential connectivities. The connectivity between the $C^{\alpha}H$ proton of Leu-70 and NH of Ile-71 allowed the identification of the latter residue, but only its NH and $C^{\alpha}H$ could be detected in the fingerprint region. The broadness of the signals corresponding to the Asn-72 side-chain protons and the atypical chemical shifts of its terminal NH protons are also of note (Table I).

In the same region, a slight discrepancy has been noticed between the published primary sequence of the protein (Tedro et al., 1981) and the sequence read from 2D NMR data. Residue 74 was expected to be Asp (Tedro et al., 1981), but the spin system associated with this residue clearly shows NOESY cross peaks between the β-protons and two additional protons compatible with the carboxamide group of an Asn (Figure 4). These features were further borne out by the observation of a NOESY cross peak between these carboxamide protons (Figure 4). Overall, the NMR data strongly suggest that residue 74 is an Asn as initially proposed (Dus et al., 1973) rather than an Asp as latter suggested (Tedro et al., 1981). The nature of this residue has been positively identified by amino acid sequencing of the tryptic peptide spanning residues 70–83; the fifth cycle of sequencing for this peptide gave a definite increase in the Asn value compared to Asp, which clearly indicates that residue 74 is indeed Asn in the samples used in this work.

The last five residues of the sequence were identified in reverse order, starting with Gly-85. The signals of the two $C^{\alpha}H$ protons of this residue are nearly degenerate, and the amide resonance was sharper than those of the other amino acids.

A spin system showing protons on only one carbon atom of the side chain, with broad lines and a NH proton at 8.13 ppm, has been observed; since NOESY spectra have also indicated the presence of carboxamide protons, this set has been attributed to Asn-45, the only remaining Asn of the sequence.

At this stage, only localized portions of the molecule remained unassigned. First, no clear signature of the N-terminal

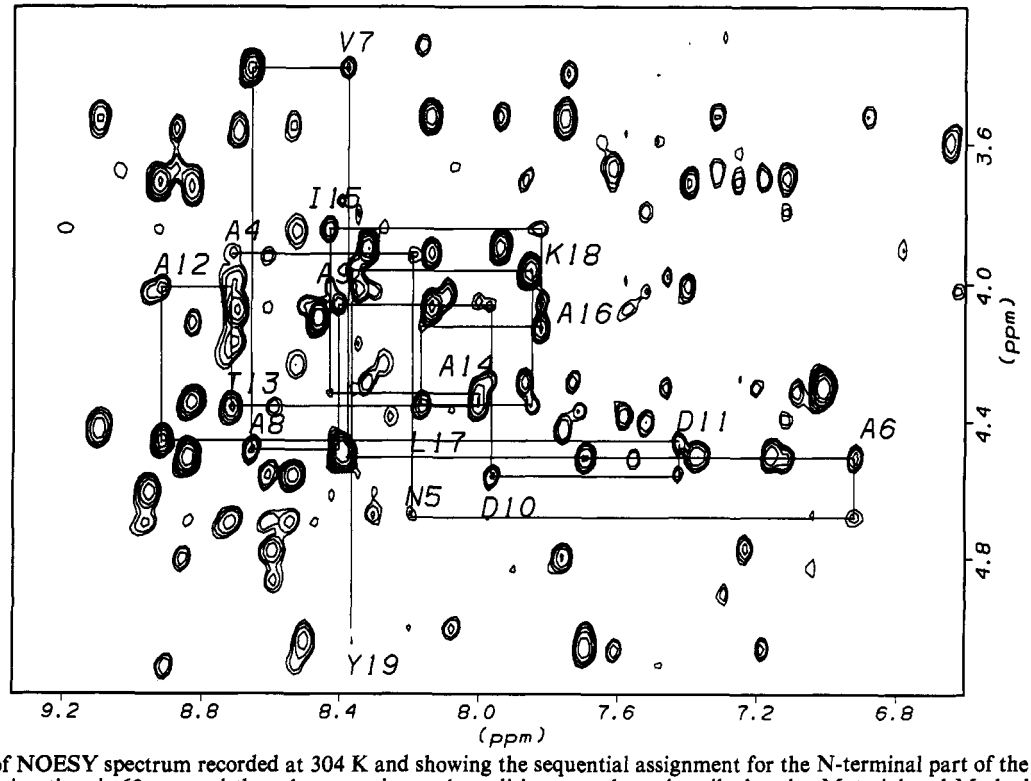

FIGURE 2: Part of NOESY spectrum recorded at 304 K and showing the sequential assignment for the N-terminal part of the reduced HiPIP protein. The mixing time is 60 ms, and the other experimental conditions are those described under Material and Methods.

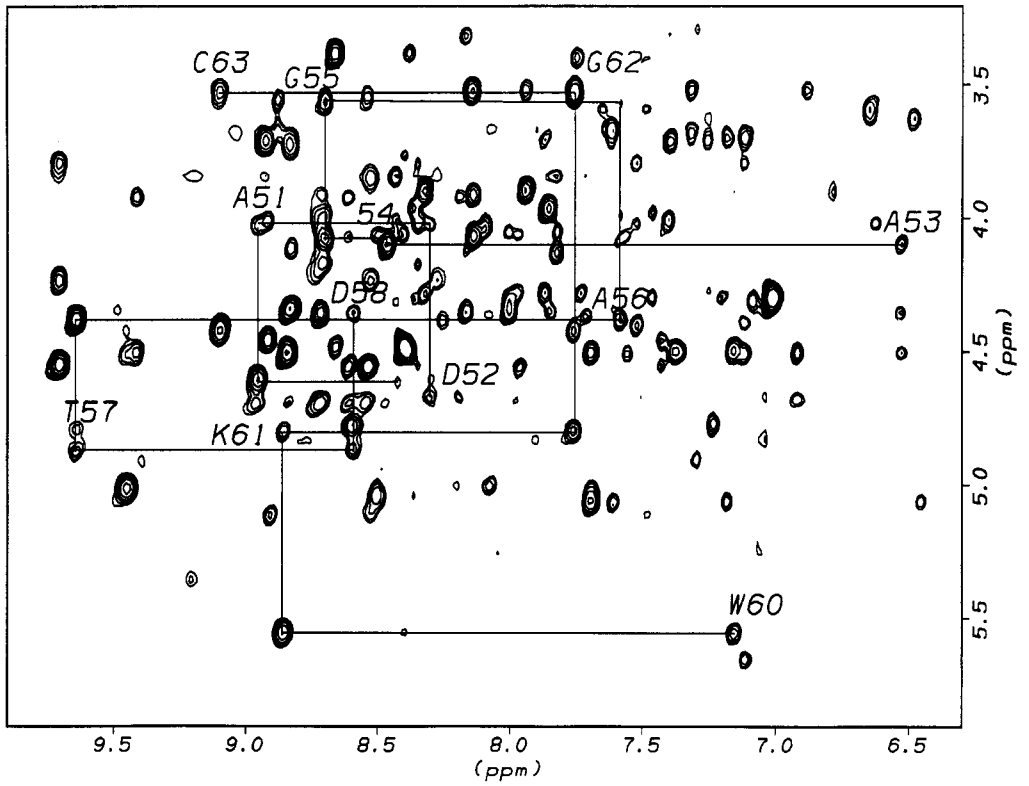

FIGURE 3: Part of NOESY spectrum showing sequential assignments for residues 50–63. Conditions are the same as in Figure 2.

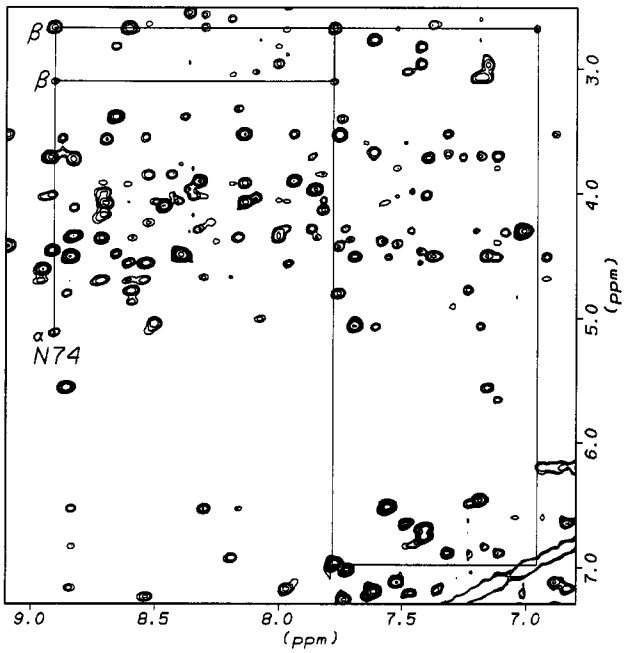

FIGURE 4: Part of NOESY spectrum showing intraresidue proton NOESY cross peaks for Asn-74, including carboxamide protons. Conditions are the same as in Figure 2.

dipeptide has been observed, and this part of the sequence will not be further discussed here. The NOESY cross peak at 4.22 ppm between the $C^{\alpha}H$ of Pro-3 and NH of Ala-4 has allowed us to get the position of the resonances arising from the first proline of the sequence. Then three other segments, Cys-43–Met-49, Cys-63–Phe-66, and Trp-76–Trp-80, involve residues neighboring the ligands of the iron–sulfur cluster. Due to the proximity of the paramagnetic center, it is not straightforward with standard 2D NMR experiments to assign these protons. This explains our failure to identify the three amino acids on the carboxy side of each cysteine ligand. In order to circumvent these difficulties and to detect correlations between very fast relaxing signals, special experiments involving COSY with fast repetition times (80 ms), HOHAHA with reduced spin-lock duration (30 ms and below), and NOESY with very short mixing times (15 ms) were carried out.

Using the spectra thus recorded, additional assignments could be achieved. The Cys-43 NH at 9.22 ppm was identified by its NOESY cross peaks with His-42 $C^{\alpha}H$ and with one of the His-42 $C^{\beta}H$. In addition, a weak COSY signal (9.22–4.82 ppm) could be attributed to the NH–$C^{\alpha}H$ correlation of Cys-43. The assignments for $C^{\alpha}H$ (4.3 ppm) and $C^{\beta}H$ (10.16 and 11.13 ppm) of Cys-46 have been recently proposed (Bertini et al., 1992). Hence, the unassigned COSY cross peak at 8.14–4.25 ppm is a good candidate for the NH–$C^{\alpha}H$ *J*-correlation of this residue. The same signal was correlated with a NOESY peak at 8.79–4.25 ppm which may be used to assign Gln-47 NH and then the associated spin system identified in COSY spectra (Table I). NOESY cross peaks between $C^{\alpha}H$ of Gly-62 and NH of Cys-63 have provided a firm assignment for the latter residue, which is corroborated by the COSY correlation between NH and $C^{\alpha}H$ of Cys-63 at 9.15–3.73 ppm. In addition, a NOESY cross peak at 9.08–3.73 ppm which may arise from the correlation between $C^{\alpha}H$ of Cys-63 and NH of Gln-64 has been detected. At the corresponding NH position, a spin system compatible with Gln-64 was found. Also noticeable was the existence of two NOESY cross peaks which may correlate both $C^{\alpha}H$ of Gly-75 with the NH of Trp-76. However, it has not been possible to detect a spin system associated with the latter NH. NOESY cross peaks at 12.62–7.61 and 8.32–7.61 ppm (at 304 K) were attributed to the coupling between one $C^{\beta}H$ and the NH of Cys-77, as well as that between $C^{\alpha}H$ and the same NH based on the available assignments for these side-chain protons (Bertini et al., 1992).

The positions of the two spin systems corresponding to the ring protons of Trp-76 and Trp-80 have been observed in

Table I: ^{1}H Resonance Assignments of Reduced HiPIP Ferredoxin Chemical Shift (ppm)[a]

residue	NH	$C^{\alpha}H$	$C^{\beta}H$	others
Ser-1				
Ala-2				
Pro-3		4.22	2.19, 1.57	
Ala-4	8.70	3.97	1.38	
Asn-5	8.24	4.73	3.11, 2.67	$N^{\delta}H$ 7.24, 6.5
Ala-6	6.97	4.56	0.82	
Val-7	8.43	3.45	1.20	$C^{\gamma}H$ 0.24, 0.04
Ala-8	8.68	4.55	1.56	
Ala-9	8.43	4.13	1.46	
Asp-10	8.01	4.61	2.94, 2.56	
Asp-11	7.49	4.53	3.01, 2.88	
Ala-12	8.93	4.07	1.56	
Thr-13	8.76	4.11	4.41	$C^{\gamma}H$ 1.13
Ala-14	8.07	4.36	1.78	
Ile-15	8.47	3.91	1.88	$C^{\gamma}H_3$ 0.99; $C^{\gamma}H_2$ 1.21; $C^{\delta}H$ 0.9
Ala-16	7.86	4.18	1.61	
Leu-17	8.19	4.41	2.08, 2.34[b]	$C^{\gamma}H$ 2.05
Lys-18	7.91	4.02	2.33, 2.08	$C^{\gamma}H$ 1.42; $C^{\delta}H$ 1.80; $C^{\epsilon}H$ 3.03
Tyr-19	8.40	5.10	3.01, 2.60	$C^{\epsilon}H$ 6.70; $C^{\delta}H$ 6.99
Asn-20	8.51	4.13	2.26	$N^{\delta}H$ 7.62, 6.56
Gln-21	8.20	3.99	2.03, 2.45	$C^{\gamma}H$ 2.45, 2.18; $N^{\epsilon}H$ 7.78, 7.06
Asp-22	8.65	4.61	2.73, 2.36	
Ala-23	9.74	3.87	1.65	
Thr-24	8.41	4.08	4.23	$C^{\gamma}H$ 1.27
Lys-25	7.57	4.46	1.64, 2.08	$C^{\gamma}H$ 1.35; $C^{\delta}H$ 1.21; $C^{\epsilon}H$ 2.94
Ser-26	7.17	4.57	3.76, 5.70	
Glu-27	8.87	4.41	1.87	$C^{\gamma}H$ 2.54, 2.37
Arg-28	6.64	3.01	2.04, 3.01	$C^{\gamma}H$ 0.84, 0.55; $C^{\delta}H$ 0.55, −0.73
Val-29	8.17	3.38	1.85	$C^{\gamma}H$ 0.82
Ala-30	7.42	4.06	1.41	
Ala-31	8.13	4.13	1.75	
Ala-32	7.45	3.79	1.34	
Arg-33	10.5	4.50	2.47, 2.25	$C^{\gamma}H$ 2.09
Pro-34		4.64	2.07	$C^{\delta}H$ 3.97, 3.85
Gly-35	8.55	4.74, 3.61		
Leu-36	7.28	4.83	1.50	$C^{\gamma}H$ 1.12
Pro-37		4.63	2.45, 1.36	$C^{\gamma}H$ 1.98; $C^{\delta}H$ 3.84, 3.50
Pro-38		4.58		$C^{\delta}H$ 3.92, 3.77
Glu-39	8.94	3.63	1.86, 1.96	$C^{\gamma}H$ 2.05, 2.15
Glu-40	7.77	4.15	1.94, 1.74	$C^{\gamma}H$ 2.34, 2.12
Gln-41	7.33	3.77	1.70, 0.22	$C^{\gamma}H$ 1.86, −0.05; $N^{\epsilon}H$ 6.70, 6.50
His-42	9.00	6.23	3.96, 3.88	
Cys-43	9.22	4.82		
Ala-44	7.73	3.69	1.30	
Asn-45	8.13	5.06	3.72, 2.83	$N^{\delta}H$ 7.66, 7.24
Cys-46	8.14	4.25[c]		
Gln-47	8.79	4.05	0.69	$C^{\gamma}H$ 1.61, 1.70
Phe-48	7.82	3.60	3.50, 2.27	$C^{\delta}H$ 7.16; $C^{\epsilon}H$ 7.36
Met-49				
Gln-50	8.44	4.64	1.61, 1.85	$C^{\gamma}H$ 2.22, 2.30
Ala-51	8.95	4.09	1.44	
Asp-52	8.34	4.74	2.73, 2.58	
Ala-53	6.59	4.17	1.28	
Ala-54	8.47	4.13	1.26	
Gly-55	8.72	4.05, 3.63		
Ala-56	7.63	4.43	1.61	
Thr-57	9.66	4.83	4.93	$C^{\gamma}H$ 1.40
Asp-58	8.63	4.41	2.73, 2.36	
Glu-59	8.03	4.34	1.75, 1.65	$C^{\gamma}H$ 1.98
Trp-60	7.22	5.62	3.14, 2.98	$C^{\delta}H$ 7.20; $N^{\epsilon}H$ 10.08; $C^{\zeta}H$ 7.48; $C^{\eta}H$ 7.36; $C^{\eta}H$ 7.21
Lys-61	8.90	4.85	1.62, 1.66	$C^{\gamma}H$ 1.99
Gly-62	7.81	4.49, 3.58		
Cys-63	9.15	3.73		
Gln-64	9.08		2.21,[b] 1.98[b]	
Leu-65				
Phe-66	7.35	4.97	2.72, 2.32	$C^{\epsilon}H$ 7.84,[c] $C^{\delta}H$ 7.10[c]
Pro-67		4.39	2.30, 1.95	$C^{\gamma}H$ 2.10; $C^{\delta}H$ 3.59, 3.37
Gly-68	8.84	4.17, 3.79		
Lys-69	7.67	5.13	1.55, 1.88	$C^{\gamma}H$ 1.33; $C^{\delta}H$ 1.55; $C^{\epsilon}H$ 2.98
Leu-70	7.75	5.08	1.14, 1.62	$C^{\gamma}H$ 1.28; $C^{\delta}H$ 0.54, 0.69
Ile-71	9.53	4.57		
Asn-72	7.44	4.55	2.69, 1.71	$N^{\delta}H$ 9.46, 6.55
Val-73	8.44	3.82	2.15	$C^{\gamma}H$ 1.00
Asn-74	8.98	5.18	3.17, 2.73	$N^{\delta}H$ 7.82, 7.02
Gly-75	8.58	4.33, 3.90		
Trp-76	8.34	3.96	2.98, 1.60	$C^{\delta}H$ 6.78; $N^{\epsilon}H$ 9.83; $C^{\zeta}H$ 7.48; $C^{\zeta}H$ 6.83; $C^{\epsilon}H$ 7.17; $C^{\eta}H$ 6.65
Cys-77	7.61			

Table I (Continued)

residue	NH	$C^{\alpha}H$	$C^{\beta}H$	others
Ala-78				
Ser-79				
Trp-80	7.60	6.60	3.09	$C^{\delta}H$ 8.93; $N^{\epsilon}H$ 10.53; $C^{\zeta}H$ 7.32; $C^{\zeta,\eta}H$ 7.21, 7.12
Thr-81	6.50	3.99	3.11	$C^{\gamma}H$ 0.79
Leu-82	7.98	3.61	1.64, 1.46	
Lys-83	8.17	3.99	1.60, 1.28	
Ala-84	8.37	4.36	1.37	
Gly-85	7.90	3.75		

[a] Chemical shift at 308 K (304 K for the ring protons) and pH 6 with an accuracy of ±0.02 ppm. [b] Proton belonging to the spin system of the residue and whose assignment is only tentative. [c] Assignments taken from Bertini et al. (1992).

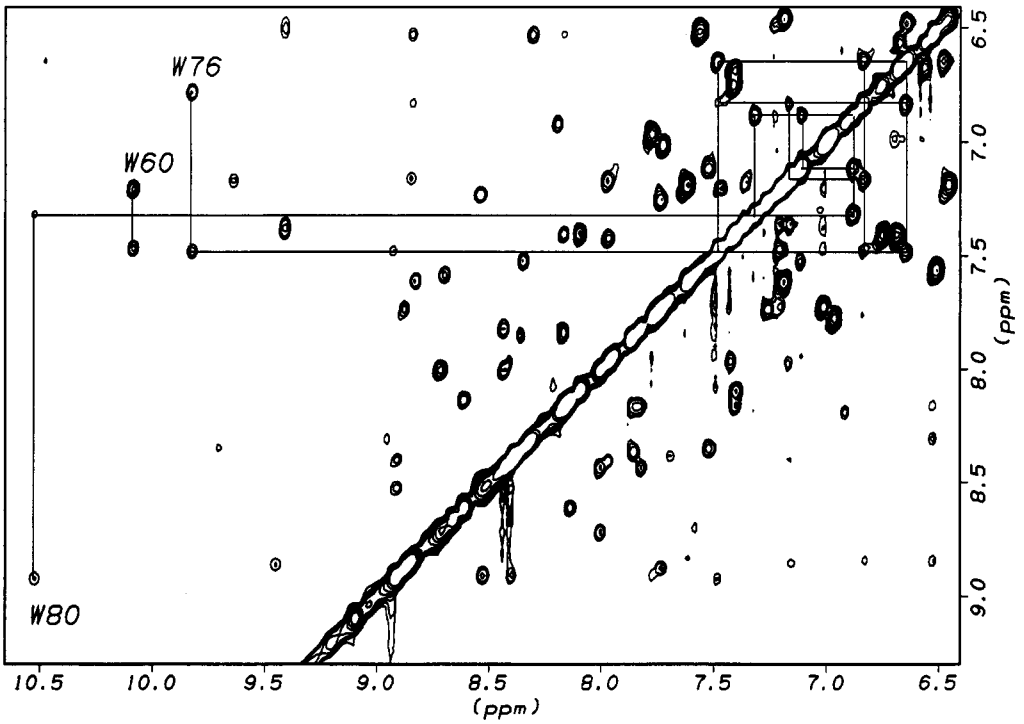

FIGURE 5: Part of NOESY spectrum showing the cross peaks between the ring NH of the Trp and the two nearest neighbors on the same residue. The connections with the other ring protons are given for Trp-76 and Trp-80. Conditions are the same as in Figure 2.

COSY and NOESY spectra in D_2O and H_2O (Figure 5). Since no sequential cross peak involving any of these two residues was detected in the present set of experiments, the strong NOESY interaction between the protons of Gln-41 and one ring NH has been used to distinguish between them. The results of X-ray crystallography (Carter et al., 1974) predicted the two $C^{\beta}H$ of Gln-41 to be at 2.15 and 3.26 Å from the ring NH of Trp-76 and may explain the two correlations observed between this NH and the $C^{\beta}H$ of Gln-41. Three NOESY cross peaks involving the ring singlet of Trp-76 were observed at 3.96, 2.98, and 1.60 ppm. These peaks are attributed to the interaction of the ring singlet proton with the side-chain protons of Trp-76. No NOESY cross peak involving the ring singlet of Trp-80 which would define its side chain has been detected. However, a NOESY cross peak relates the signal of the NH ring proton of Trp-76 with a resonance at 3.09 ppm which, on the basis of the crystallographic results (Carter et al., 1974), may correspond to one $C^{\beta}H$ of Trp-80.

The observation of an interaction between the para-proton of a Phe and one hyperfine-shifted $C^{\beta}H$ of a Cys has led to the assignment of these signals to residues 66 and 63, respectively (Bertini et al., 1992), again on the basis of the crystallographic structure (Carter et al., 1974). In our experiments, COSY spectra provided the correlation between the ortho- and meta-protons of Phe-66, but no NOESY cross peak between the ortho-protons and the $C^{\beta}H$ has been observed. In the D_2O COSY spectra, one unassigned cross peak in the aromatic region remained which was consistent with the coupling of the ortho- and meta-protons of another Phe residue. A NOESY cross peak was observed between these ortho-protons and one proton of a spin system with its NH at 7.82 ppm. This last spin system was assigned to Phe-48 (Table I).

At this point, seven residues were left completely unidentified: Ser-1, Ala-2, Ala-44, Met-49, Leu-65, Ala-78, and Ser-79. It is of note here that the NH of two of these (Leu-65 and Ser-79) have been proposed to be hydrogen bonded by $S\gamma$ atoms of the cluster on the basis of X-ray crystallographic analysis (Carter et al., 1974). Among the remaining unassigned signals, a spin system displaying a single carbon atom in the side chain was found to have a slow-exchanging NH at 7.35 ppm and broad resonances, all features characteristic of a residue in the vicinity of the iron–sulfur center. In the D_2O NOESY spectra, two cross peaks connecting the $C^{\alpha}H$ of this spin system with protons identified as $C^{\delta}H$ of proline were observed, allowing us to identify the Phe-66–Pro-67 pair. Other spin systems were observed, among which at least one at a NH position of 7.73 ppm is consistent with an alanine residue. A NOESY cross peak between the methyl group of this residue and the NH of Asn-45 has been detected; despite the absence of other sequential peaks, these associated features may be assigned to the Ala-44–Asn-45 junction between the

first two cysteines of the sequence.

The rates of exchange for NH protons have been evaluated by recording spectra at increasing time intervals (between a few hours and several weeks) after a freeze-dried sample of reduced HiPIP was dissolved in D_2O. Figure 1 lists the residues which have the slowest exchanging NHs. Some of them are known from the X-ray structure (Carter et al., 1974) to belong to the hydrophobic core surrounding the metallic cluster. It is the case of the protons of Asn-45, Trp-60, Lys-61, Phe-66, Leu-70, Ile-71, Asn-72, and Gly-75 which are the most resistant to D/H exchange: their NH protons exchange on a time scale of months as already qualitatively reported (Orme-Johnson et al., 1983; Backes et al., 1991).

Discussion

The 2D NMR experiments reported herein have provided the assignments for a large majority of the protons of *C. vinosum* HiPIP, since protons of 79 amino acids out of the 85 residues in the sequence have been identified in the spectra (Table I). These data might have been somewhat unexpected as the presence of the iron–sulfur center is generally thought to perturb the relaxation properties of the neighboring protons and to interfere with the detection of NOESY and COSY cross peaks. In the case of iron–sulfur proteins, the only example so far of complete assignments has been conducted on the [2Fe–2S] ferredoxin from *Anabaena* using both homo- and heteronuclear 2D NMR (Oh & Markley, 1990a,b; Skjeldal et al., 1990). Adequate methodology to deal with fast-relaxing protons has been devised (Skjeldal et al., 1991, and references herein) but cannot be used to carry out all the assignments for a protein the size of *C. vinosum* HiPIP. Hence, it is worth analyzing the present set of experiments based on conventional protein 2D NMR (Wüthrich, 1986) to determine to what extent and by what means the complete attribution of ^1H NMR signals can be reached for a [4Fe–4S] protein, an heretofore uncompleted task.

Amino Acids with Broadened or Shifted Signals. Among the amino acids identified in the NMR spectra, some display an unusual set of resonances. For instance, the signals associated with Gln-41 are shifted upfield: on the basis of the results of X-ray crystallography (Carter et al., 1974), it is worth noticing that this residue is, on one hand, involved in hydrogen bonding to an internal water molecule through its carboxamide oxygen and, on the other hand, facing the Trp-80 aromatic ring. Similarly, Arg-28 seems to be hydrogen bonded to the same water molecule by its backbone carbonyl and to interact with Trp-76; the associated set of chemical shifts is accordingly rather unusual.

Other spin systems, for example Tyr-19 or Asn-72, have significantly broadened signals, most probably through interactions with the paramagnetic center. In other instances, some correlations are missing, as in the case of the spin system assigned to Ile-71. These residues have been shown by X-ray crystallography (Carter et al., 1974) to lie in the vicinity of the iron–sulfur cluster. However, a remarkable trend of the assignments reported here is that nearly all spin systems have been identified, although incompletely in some cases, while a larger proportion of the sequential NOESY cross peaks has remained undetected. The present observation is to be compared with that displayed by *Anabaena* 7120 [2Fe–2S] ferredoxin (Oh & Markley, 1990a,b; Oh et al., 1990) for which no proton closer than a weighted distance of 7.8 Å from the cluster could be observed under experimental conditions similar to those used here. In the present case of reduced *C. vinosum* HiPIP, the NH protons of all residues located between 3.7 and 6.5 Å from the nearby metal in the X-ray structure have been observed, indicating that the distance threshold for signal observations is lower than in the case of the [2Fe–2S] ferredoxin. This difference between the two types of Fe–S proteins is likely to be related to quantitative (shorter electronic relaxation for the active site of the HiPIP protein) and maybe qualitative (different spin density distributions on the clusters) differences in the relaxation processes. In the case of the HiPIP protein, the difficulty in detecting some signals and the correlations among them for the protons close to the cluster could result mainly from the overlap of these relatively broad signals with other resonances not perturbed or less perturbed by the electronic spin. Accordingly, correlations have been detected among cysteinyl protons, which are the fastest relaxing protons in the protein but whose signals are shifted out of the diamagnetic range. Along the same lines, we suspect that the residues involved in hydrogen bonding to the Sγ atoms of the ligands, Leu-65 or Ser-79, either have remained undetected because they are hidden by the sharper signals of the diamagnetic envelope or have their NOESY cross peaks blurred because the signals are broad and fall in the same region.

Elements of Secondary Structure. The NH–NH correlations reported in Figure 1 are a good indicator of the presence of α-helices. Two segments of amino acids fulfill the requirements for such a structural motif. The first one apparently spans the segment Ala-12–Tyr-19. X-ray crystallographic analysis (Carter et al., 1974) limited the α-helix in this region to Ala-16, and the observation of a strong NH–NH NOE extending to residue 19 may be due to the occurrence of a turn followed by an element of left-handed helix at residue 18 as concluded from the X-ray results (Carter et al., 1974). The second α-helix involves residues 28–32; here also, as in the first instance, the last residue of the segment has dihedral angles in the crystallographic structure indicative of a left-handed helix (Carter et al., 1974), and the NH–NH correlations extend beyond the crystallographically determined α-helix. Some of the hairpin turns evidenced by X-ray crystallography can be identified by the characteristic NH–NH correlations they give in the NMR spectra; this is especially the case for those involving residues 5–6, 9–11, 21–22, 24–26, 39–41, 55–56, 59–60, 68–69, and 73–75.

The largest remarkable element of secondary structure observed by X-ray crystallography (Carter et al., 1974) is the twisted antiparallel β-sheet enclosing the iron–sulfur cluster binding region (residues 48–75). NMR spectra provide a confirmation of the occurrence of the β-sheet in solution; first, all NHs expected to participate in hydrogen bonding to main chain carbonyl oxygens (Carter et al., 1974) have been found to exchange slowly with D_2O, with the exception of the NH of Ala-56. Second, clear NOEs have been observed between the NH of Lys-61 and Ile-71 involved in the β-sheet, although the NOE between the protons of Gly-62 and Gln-50 has escaped detection. The precise structure of the β-sheet might thus be slightly different in solution and in the crystal.

NMR spectra also provide evidence, through the long-range interresidue NOE between the NH of Val-7 and Leu-70, that the N-terminal part of the molecule remains in close contact in solution with part of the β-turn, at the so-called intramolecular interface noticed by X-ray crystallography (Carter et al., 1974).

A more detailed analysis of the intramolecular interactions in *C. vinosum* HiPIP is premature in view of the uncertainty linked to the positions of a few protons of the molecule. The use of heteronuclear multidimensional NMR methods and of experiments more appropriate for the detection of fast-relaxing

signals will undoubtedly provide a more extensive set of assignments. It is, however, striking that the conventional approach for resonance assignments used here has succeeded in locating the spectroscopic signature of more than 90% of the amino acids building the complete sequence, despite the presence of the paramagnetic active site. This result is encouraging with respect to the possibility of analyzing the complete NMR spectra of the oxidized form of the same protein and to provide in depth information on the events occurring at the atomic level upon electron transfer, a matter of intense interest (Moulis et al., 1988; Backes et al., 1991) and yet poorly understood.

Added in Proof

While this work was under review, a paper (Nettesheim et al., 1992) was published which gives the assignments of cysteine protons and other sequential assignments for the same protein at the oxidized level. It is interesting to note that for most residues identified in both the latter paper and the work reported here, the assigned resonance frequencies are in close agreement. Differences, which appear too large to arise from variations in experimental conditions, are observed for a few residues in the vicinity of the active site. Although such differences are not unexpected due to the different electronic states of the iron–sulfur cluster in the two redox levels of the protein, they should be assessed under a strict control of the experimental conditions before they can be fully appreciated.

Acknowledgments

We are grateful to Dr. B. Lamotte for his continuous encouragements and to Dr. J. Meyer for careful reading of the manuscript and useful suggestions. We thank Professor I. Bertini and his co-workers for access to their work on some assignments prior to publication. The assistance of M. F. Foray was very helpful to run the 600-MHz spectrometer of the Institut de Biologie Structurale. The amino acid sequencing has been carried out by Dr. J. Gagnon and N. Scherrer, who are gratefully acknowledged. Dr. Y. Jouanneau is also thanked for access to his large-scale fermentation equipment and Dr. D. Marion for advice on the HOHAHA experiments.

Registry No. Asn, 70-47-3.

References

Backes, G., Mino, Y., Loehr, T. M., Meyer, T. E., Cusanovich, M. A., Sweeney, W. V., Adman, E. T., & Sanders-Loehr, J. (1991) *J. Am. Chem. Soc. 113*, 2055–2064.

Bartsch, R. G. (1978) *Methods Enzymol. 53B*, 329–340.

Bax, A. (1989) *Methods Enzymol. 176A*, 151–168.

Bax, A., & Davis, D. G. (1985) *J. Magn. Reson. 65*, 355–360.

Bertini, I., Briganti, F., Luchinat, C., Scozzafava, A., & Sola, M. (1991) *J. Am. Chem. Soc. 113*, 1237–1245.

Bertini, I., Capozzi, F., Ciurli, S., Luchinat, C., Messori, L., & Piccioli, M. (1992) *J. Am. Chem. Soc. 114*, 3332–3340.

Breiter, D. R., Meyer, T. E., Rayment, I., & Holden, H. M. (1991) *J. Biol. Chem. 266*, 18660–18667.

Carter, C. W., Jr., Kraut, J., Freer, S. T., Xuong, N.-H., Alden, R. A., & Bartsch, R. G. (1974) *J. Biol. Chem. 249*, 4212–4225.

Carter, C. W., Jr. (1977) in *Iron–Sulfur Proteins* (Lovenberg, W., Ed.) Vol. III, pp 158–204, Academic Press, New York.

Cowan, J. A., & Sola, M. (1990) *Biochemistry 29*, 5633–5637.

Dugad, L. B., LaMar, G. N., & Unger, S. W. (1990) *J. Am. Chem. Soc. 112*, 1386–1392.

Dus, K., Tedro, S. M., & Bartsch, R. G. (1973) *J. Biol. Chem. 248*, 7318–7331.

Krishnamoorthi, R., Markley, J. L., Cusanovich, M. A., Przysiecki, C. T., & Meyer, T. E. (1986) *Biochemistry 25*, 60–67.

Krishnamoorthi, R., Cusanovich, M. A., Meyer, T. E., & Przysiecki, C. T. (1989) *Eur. J. Biochem. 181*, 81–85.

Macura, S., Huang, Y., Suter, D., & Ernst, R. R. (1981) *J. Magn. Reson. 43*, 259–281.

Malik, K. A. (1983) *J. Microbiol. Methods 1*, 343–352.

Middleton, P., Dickson, D. P. E., Johnson, C. E., & Rush, J. D. (1980) *Eur. J. Biochem. 104*, 289–296.

Moulis, J.-M., Lutz, M., Gaillard, J., & Noodleman, L. (1988) *Biochemistry 27*, 8712–8719.

Nettesheim, D. G., Meyer, T. E., Feinberg, B. A., & Otvos, J. D. (1983) *J. Biol. Chem. 258*, 8235–8239.

Nettesheim, D. I., Harder, S. R., Feinberg, B. A., & Otvos, J. D. (1992) *Biochemistry 31*, 1234–1244.

Oh, B.-H., & Markley, J. L. (1990a) *Biochemistry 29*, 3993–4004.

Oh, B.-H., & Markley, J. L. (1990b) *Biochemistry 29*, 4012–4017.

Oh, B.-H., Mooberry, E. S., & Markley, J. L. (1990) *Biochemistry 29*, 4004–4011.

Orme-Johnson, N. R., Mims, W. B., Orme-Johnson, W. H., Bartsch, R. G., Cusanovich, M. A., & Peisach, J. (1983) *Biochim. Biophys. Acta 748*, 68–72.

Plateau, P., & Guêron, M. (1982) *J. Am. Chem. Soc. 104*, 7310–7311.

Przysiecki, C. T., Meyer, T. E., & Cusanovich, M. A. (1985) *Biochemistry 24*, 2542–2549.

Rance, M., Sorensen, O. W., Bodenhausen, G., Wagner, G., Ernst, R. R., & Wüthrich, K. (1987) *Biochem. Biophys. Res. Commun. 117*, 479–485.

Skjeldal, L., Westler, W. M., Oh, B. H., Krezel, A. M., Holden, H. M., Jacobson, B. L., Rayment, I., & Markley, J. L. (1991) *Biochemistry 30*, 7363–7368.

Skjeldal, L., Westler, W. M., & Markley, J. L. (1990) *Arch. Biochem. Biophys. 278*, 482–485.

States, D. J., Haberkorn, R. A., & Ruben, D. J. (1982) *J. Magn. Reson. 48*, 286–292.

Tedro, S. M., Meyer, T. E., Bartsch, R. G., & Kamen, M. D. (1981) *J. Biol. Chem. 256*, 731–735.

Tedro, S. M., Meyer, T. E., & Kamen, M. D. (1985) *Arch. Biochem. Biophys. 241*, 656–664.

Wüthrich, K. (1986) *NMR of Proteins and Nucleic Acids*, John Wiley, New York.